HIGHLY AUTOMATED OPTICAL CHARACTERIZATION
WITH FTIR SPECTROMETRY

By G.L.E. Perry and F. R. Szofran

Space Science Laboratory
Science and Engineering Directorate

September 1989

1. REPORT NO. NASA TM- 100379	2. GOVERNMENT ACCESSION NO.	3. RECIPIENT'S CATALOG NO.
4. TITLE AND SUBTITLE Highly Automated Optical Characterization with FTIR Spectrometry		5. REPORT DATE September 1989
		6. PERFORMING ORGANIZATION CODE ES75
7. AUTHOR(S) G.L.E. Perry and F. R. Szofran		8. PERFORMING ORGANIZATION REPORT #
9. PERFORMING ORGANIZATION NAME AND ADDRESS George C. Marshall Space Flight Center Marshall Space Flight Center, AL 35812		10. WORK UNIT, NO.
		11. CONTRACT OR GRANT NO.
		13. TYPE OF REPORT & PERIOD COVERED
12. SPONSORING AGENCY NAME AND ADDRESS National Aeronautics and Space Administration Washington, DC 20546		Technical Memorandum
		14. SPONSORING AGENCY CODE

15. SUPPLEMENTARY NOTES

Prepared by Space Science Laboratory, Science and Engineering Directorate

16. ABSTRACT

The procedure for evaluating the characteristics of II-VI semiconducting infrared sensor materials with a Fourier Transform Infrared (FTIR) spectrometer system will be discussed. While the method of mapping optical characteristics with a spectrometer has been employed previously, this system is highly automated compared to other systems where the optical transmission data are obtained using a FTIR system with a small stationary aperture in the optical path and moving the specimen behind the aperture. The hardware and software, including an algorithm developed for extracting cut-on wavelengths of spectra, as well as several example results, will be described to illustrate the advanced level of the system. Additionally, data from transverse slices and longitudinal wafers of the aforementioned semiconductors will be used to show the accuracy of the system in predicting trends in materials such as shapes of growth interfaces and compositional uniformity.

17. KEY WORDS Infrared Sensor Fourier Transform Infrared Spectrometer Optical Characterization Semiconductor Cut-On Wavelength	18. DISTRIBUTION STATEMENT Unclassified—Unlimited

19. SECURITY CLASSIF. (of this report) Unclassified	20. SECURITY CLASSIF. (of this page) Unclassified	21. NO. OF PAGES 21	22. PRICE NTIS

MSFC - Form 3292 (Rev. December 1972)   For sale by National Technical Information Service, Springfield, Virginia 22151

ACKNOWLEDGEMENTS

TABLE OF CONTENTS

iii

LIST OF ILLUSTRATIONS

LIST OF TABLES

HIGHLY AUTOMATED OPTICAL CHARACTERIZATION WITH FTIR SPECTROMETRY

INTRODUCTION

When characterizing crystals for infrared sensor applications, it is important to establish quantitatively the spatial uniformity of properties affecting the response to the infrared phonons. Optical characterization using infrared transmission edge mapping is of particular interest for alloy semiconductors such as $Hg_{1-x}Cd_xTe$ because the transmission edge is directly related to the composition of the alloy. While the method of obtaining optical spatial characteristics by using a small aperture in the optical path and moving the specimen behind the aperture has been employed previously (see reference [1]), a facility with advanced capabilities has been developed. The capabilities of the facility in addition to its associated hardware and software will be discussed. Moreover, the facility will be shown to be useful in assessing the correlation between the crystal growth parameters and the compositional redistribution during the solidification of narrow band-gap semiconductors.[2] In this laboratory, II-VI alloy semiconductors are grown from the melt by directional solidification [2-4] and quenching.[5,6] Several results of the transmission edge mapping technique have been helpful in clarifying the fluid flow phenomena occurring during these crystal growth procedures, and the internal temperature gradients [7] and effective diffusion coefficients [8-11] have been estimated in the alloy melts. Some of these results will be demonstrated with spatial maps of optical properties such as composition.

HARDWARE

The equipment for the facility is a Mattson Instruments, Inc. Sirius 100 Fourier Transform Infrared (FTIR) spectrometer system. The spectrometer includes an x-y stage which allows for desired areas of the sample to be scanned with minimal operator input. The sample is placed in front of a pinhole aperture, and the optical beam is focussed to an area 250 μm in diameter at the aperture to maximize the power to the sample. The metal foil containing the aperture does not actually touch the sample, but stays a few micrometers ahead of the sample in the optical path.[12]

The spectrometer is currently set up to operate in the mid-infrared region (2-15 μm) to accumulate optical transmission data but may be set up for other capabilities. In general, the system may be used to acquire reflection as well as transmission data through near-, mid-, and far-infrared regions. Useful spectra have been obtained in the mid-infrared range with apertures as small as 25 μm in diameter; however, the results shown in this report were all obtained with a 100 μm aperture which gave the optimum compromise between spatial resolution and the time required to obtain spectra with satisfactory signal-to-noise ratios. The beam of the signal sent through the sample is focussed and detected by a bulls-eye mercury cadmium telluride detector which is cooled at liquid nitrogen temperature to detect photon excitations. Since a small aperture is used, all signals fall on the central part of the detector. Only the central part is used so that signal-to-noise is increased over what would be obtained with the entire detector.[12]

The detector, beam splitter, and infrared source may be changed as necessary to match the spectral range of the spectrometer to the infrared response of the material. For the samples in this report, the infrared source was a globar which provides near-blackbody radiation, and the beam splitter was potassium bromide (KBr). The bench is equipped with a movable stage which can be moved in steps in the vertical plane by electronic stepper motors located at the base of the stage. One step is 50 µm, and it is the smallest increment the stage may move. The sample on the stage may be positioned throughout an area of 2.54 x 2.54 cm^2.

SOFTWARE

There are several software capabilities provided by the Mattson manufacturer which allow for generating a spectrum and then manipulating the spectrum to obtain specific characteristics, such as finding peaks in a spectrum, or smoothing, integrating, or differentiating a spectrum. The system makes use of a header file which includes many parameter settings for proper scanning and spectral collection. Some of the parameters include number of scans taken per point (nscans), sample shape (shape), sample size (radius for a circle or x-y coordinates for rectangular wafers), detector type (det), etc. (see sample header listing, Table 1).

Much of the software has been generated by the authors, in-house, to supplement and enhance the capabilities of the system. The spectrometers and terminals are run through a main computer by the UNIX (a trademark of AT&T Bell Laboratories) operating system. While most of the author-generated software was written in the C programming language, the UNIX system generally makes it convenient to handle unusual conditions. For example, "noisy" spectra can be smoothed and re-analyzed. Or, if the spectra contain impurity peaks such as carbon dioxide near 2350 cm^{-1} (4.26 µm) because of inadequate nitrogen purging, these peaks can easily be replaced by a straight line segment connecting any two input wavenumber points (using software provided by the spectrometer manufacturer) before the spectra are analyzed.[12] The software generated by the authors uses additions to the header files used by the standard spectrometer software (see Table 1). Software has been created to read the header file additions and move the sample with the x-y stage according to specifications. Once a spectrum is produced by performing a Fourier transformation, the cut-on wavelength is found by the following method.

Parameters are added to the header file which include *transp1, transp2, opaque1,* and *opaque2.* The first pair of parameters is set in one of two ways, described below, and is used to determine a transmittance value characteristic of each spectrum which is called *transp.* The second pair is set in a range where there is no transmittance (see O_1 and O_2 in Figure 1) and is used to determine a parameter called *opaque.* This method of designating opaque regions is used instead of merely assuming zero transmittance in the opaque spectral region to account for spectra with shifted baselines.[12] The algorithm locates the portion of a spectrum with transmittance greater than 25% and less than 75% of the span between *opaque* and *transp* and then fits a straight line to the points in that region using the method of least squares. The intercept of this line with the wavenumber axis is taken as the cut-on wavelength.

Transp is dependent on the two parameters, *transp1* and *transp2*, which are set in a range where the spectra exhibit transmission (see T_1 and T_2, Figure 1). The choice of *transp1* and *transp2* is determined by two different methods depending on the amount of free carrier absorption present in the sample. The first case involves samples with low free carrier absorption for which the transmittance is essentially constant over a substantial range beyond the cut-on. The range designated by *transp1* and *transp2* is simply averaged and this value is used as the value of *transp*. In the case of high free carrier absorption, in which the transmittance rises to a peak and then falls off immediately at lower wavenumbers, the wavenumber corresponding to the maximum transmission between *transp1* and *transp2* is located (see T_{max} in Figure 1). Then, beginning at the wavenumber for T_{max} and extending to lower wavenumbers over a range set by another additional header parameter, *dT*, the transmittance is averaged to obtain the value of *transp* (see the cross-hatched region in Figure 1).

The sample is mapped in a manner which depends on its shape. For a rectangular sample, the mapping is started in one corner and proceeds back and forth horizontally with a vertical step at the completion of each horizontal line. For circular samples, mapping begins in the center and one half is mapped. After this half is completed, the sample is returned to the center and the second half is mapped. Mapping may be specified to a small region, such as a single point or a line, or other isolated area. For a sample with at least 15% transmittance, the time required for each point is about one minute including interferogram acquisition and the fast Fourier transform (FFT). Longer times are required for samples with less transmittance. The FFT is computed, at least in part, while the next interferogram is accumulated. To minimize data storage requirements, only the processed spectra are saved.[12]

The resolution normally used to collect spectra is 8 or 16 cm^{-1}. Spectral data points computed by the FFT are equidistant in energy, and each value of resolution above corresponds to a data point spacing of 3.86 or 7.72 cm^{-1}, respectively.[12]

After samples are mapped and analyzed for cut-on wavelength, the results may be used to reveal the characteristics of the sample. For $Hg_{1-x}Cd_xTe$ samples there is a known correlation between cut-on wavelength and the composition, x, of the sample. Several spatial composition maps have been generated for this alloy from the transmission spectra obtained. For materials such as $Hg_{1-x}Zn_xSe$, the correlation between cut-on wavelength and composition is not yet as well established. Instead, spatial plots of wavenumber characteristics have been generated to show the spatial trends in wavenumber (or energy gap) of the sample. Several characteristics of a spectrum are stored in a file which includes the spectrum-file name (name identifying the sample and the coordinates at which the spectrum was taken), cut-on wavenumber value, percent transmission of the spectrum, and a composition value (if a correlation exists between wavelength and composition). This file is then used as the input for programs used to create spatial maps. Other plots may be generated to show more clearly the characteristics of a sample caused by growth conditions such as the solid-liquid interface shape during growth and thermal asymmetries in the growth furnace.

Only spectra with a *transp* value above a particular minimum (set by the additional header parameter *transmin*) are catalogued into the file used to create the maps. The minimum is usually set to eliminate spurious contribu-

tions from opaque areas of the sample or parts of the sample holder that were inadvertently included. Some low but detectable transmission may be rescanned using more scans to improve the signal-to-noise ratio and thus the spectra may be easier to analyze. Occasionally, in samples with large compositional variations (large variations in the cut-on wavenumber) and with high free carrier absorption, the values of T_1 and T_2 must be reset for different parts of the sample. This problem may be alleviated by choosing wider limits on T_1 and T_2 at the expense of slightly longer analysis time. Also, these samples usually show very low transmittance near the edges which means the associated spectra will have low signal-to-noise ratios. This particular problem has been addressed by attempting to check the signal-to-noise ratio and then, as stated above, taking additional scans if the ratio is below a preselected level. When very inhomogeneous samples are to be characterized, these problems require additional efforts for proper analysis which include manual determination of cut-on wavelengths and spectral manipulation. Computer programs will be modified to accommodate extreme cases.

RESULTS

The Mattson spectrometer has been used to characterize many bulk samples of II-VI semiconducting alloys including $Hg_{1-x}Cd_xTe$, $Hg_{1-x}Cd_xSe$, $Hg_{1-x}Zn_xTe$, and $Hg_{1-x}Zn_xSe$ grown in-house either by unidirectional solidification or casting. Several epitaxially grown and cast grown $Hg_{1-x}Cd_xTe$ samples from other labs have also been analyzed.

Figure 2 shows a spatial map of CdTe composition, x, of a 5 mm diameter cross section of a $Hg_{1-x}Cd_xTe$ ingot grown by unidirectional solidification. The data were taken on a grid 4.4 mm in diameter. The center is shown to be Hg-rich which is typical of a directionally solidified $Hg_{1-x}Cd_xTe$ sample. In addition, the map displays radial asymmetry which is caused by asymmetries in the thermal field. The Hg-rich center indicates an interface shape concave toward the solid. These illustrations provided by the spectrometer system establish the correlation between the compositional distribution of the grown crystal and the growth parameters and will provide useful information for the control of the solid-liquid interface shape and radial thermal asymmetry.

Figure 3 is a spatial map of an axially cut wafer of $Hg_{1-x}Cd_xSe$. The slab dimensions are 5 x 19.3 mm and the data were taken over an area of 4.5 x 19 mm. During growth, the furnace translation was stopped for 31 hours.[7] The map shows buildup of Cd and the flattening of the isoconcentration surfaces as the actual growth rate decreased; also, the Cd-rich center typical of unidirectionally solidified $Hg_{1-x}Cd_xSe$ alloys is apparent. From results such as this, the mechanics of growth processes may be better understood and controlled to get desired results.

As mentioned previously, a direct correlation between the transmission edge cut-on wavelength and composition has not been established for all materials. Figure 4 shows a spatial map of wavenumber for a 5 mm cross section of a unidirectionally solidified $Hg_{1-x}Zn_xSe$ ingot. The data were taken on a 4.4 mm diameter grid. Transmittance values may also be displayed by spatial maps for all samples if desired.

Other figures may be generated including three-dimensional plots and contour maps of alloys. These figures may be generated by DISSPLA (a product of Integrated Software Systems Corporation) which is available on the Marshall

Space Flight Center Engineering Analysis and Data System (EADS). Mapping data can be uploaded onto EADS. Figure 5 shows a three-dimensional plot of a $Hg_{1-x}Cd_xTe$ cross section (same cross section as in Figure 2). The plot shows the relation between the composition and the location on the sample which is related to the interface shape of the material.

A contour map of a directionally solidified $Hg_{1-x}Cd_xSe$ sample is shown in Figure 6. This map shows the Cd-rich middle typical of these samples and illustrates the trends in composition and uniformity radially on the sample cross section. Note, however, that the composition at the edges of the contour map are not necessarily the true compositions in those regions unless the sample happened to have those compositions at those points. For both the three-dimensional plots and the contour maps, the average composition is set at the edges.

Combining several average compositions from different cross sections along a directionally solidified ingot, the growth effects may be assessed axially. Figure 7 displays the change in CdTe composition, x, along the growth axis of a 12.5 cm $Hg_{1-x}Cd_xTe$ ingot which was unidirectionally solidified using a transverse magnetic field.[13] Note how well the FTIR data compare with the data taken from density measurements.

Other applications of the spectrometer's automated features have been employed for other materials, particularly with superconductivity samples and organic materials. The superconductivity samples have included compounds containing Y, Ba, Sr, Cu, and O. By modifying the compositions of the samples, the trends in infrared response were assessed along with a superconducting transition temperature that was unique to each compound.[14]

The organic compounds have included succinonitrile (SCN) in glycerol; the spectrometer was used to assess the variations in infrared response in the different growth regions of this material.[15]

The results above show that the spectrometer facility is capable of presenting data in numerous forms for analysis. However, the system is not restricted to the examples discussed. Spatial maps and other figures are available in color for easier interpretation, if desired, or compositions and other values may be plotted by number on a spatial map. Also, other optical parameters not mentioned previously (e.g., epilayer thickness derived from interference fringes) may be used for mapping. More variations for sample characterization will be innovated for the FTIR facility as new analytical requirements arise.

CONCLUSION

The FTIR spectrometer is a tool which has successfully demonstrated the capability of establishing the spatial property mapping of solid solution semiconductors. The results obtained from this system provide optical property characteristics as well as verify and complement the results from other characterization methods such as density measurements and x-ray dispersion analysis of the samples. In addition, the system provides a comprehensive, non-destructive analysis which is highly automated and takes a small amount of operator input and time.

REFERENCES

1. L. Jastrzebski, J. Lagowski, and H.C. Gatos, J. Electrochemical Soc.126 (1979) 260.

2. F.R. Szofran and S.L. Lehoczky, J. Crystal Growth 70 (1984) 349.

3. R.N. Andrews, F.R. Szofran, and S.L. Lehoczky, J. Crystal Growth 92 (1988) 445-453.

4. S.D. Cobb, R.N. Andrews, F.R. Szofran, and S.L. Lehoczky, presented at 3rd International Conference on II-VI Compounds (II-VI-87), Monterey, CA, July 1987.

5. C.-H. Su, G.L.E. Perry, F.R. Szofran, S.L. Lehoczky, Compositional Redistribution During Casting of $Hg_{0.8}Cd_{0.2}Te$, J. Crystal Growth 91 (1988) 20-26.

6. C.-H. Su, F.R. Szofran, and S.L. Lehoczky, J. Metals 37 (1985) 89 (abstract).

7. R.N. Andrews, F.R. Szofran, and S.L. Lehoczky, J. Crystal Growth 86 (1988) 100.

8. S.L. Lehoczky, and F.R. Szofran, in: Materials Processing in the Reduced Gravity Environment of Space, Ed. G.E. Rindone (North-Holland, Amsterdam, 1982).

9. S.L. Lehoczky, F.R. Szofran, and B.G. Martin, NASA CR-161598 (1980).

10. S.L. Lehoczky and F.R. Szofran, NASA CR-161949 (1981).

11. F.R. Szofran, D. Chandra, J.-C. Wang, E.K. Cothran, and S.L. Lehoczky, J. Crystal Growth 70 (1984) 343.

12. F.R. Szofran, Gretchen L.E. Perry, S.L. Lehoczky, J. Crystal Growth 86 (1988) 650-655.

13. C.-H. Su, S.L. Lehoczky and F.R. Szofran, unpublished data.

14. M.K. Wu, J.R. Ashburn, C.J. Tornj, G.L.E. Perry, F.R. Szofran, P.H. Hor, and C.W. Chu, Study of High T_c $Y(Ba_{2-x}Sr_x)Cu_3O_y$ Compound System, Eds. D.B. Gubser, and M. Schluter, Proceedings of MRS Symposium on High Temperature Superconductors (1987) 69.

15. W.F. Kaukler, P.A. Curreri, NASA TM-100317 (1987).

HgCdSe With 100 μm Aperture
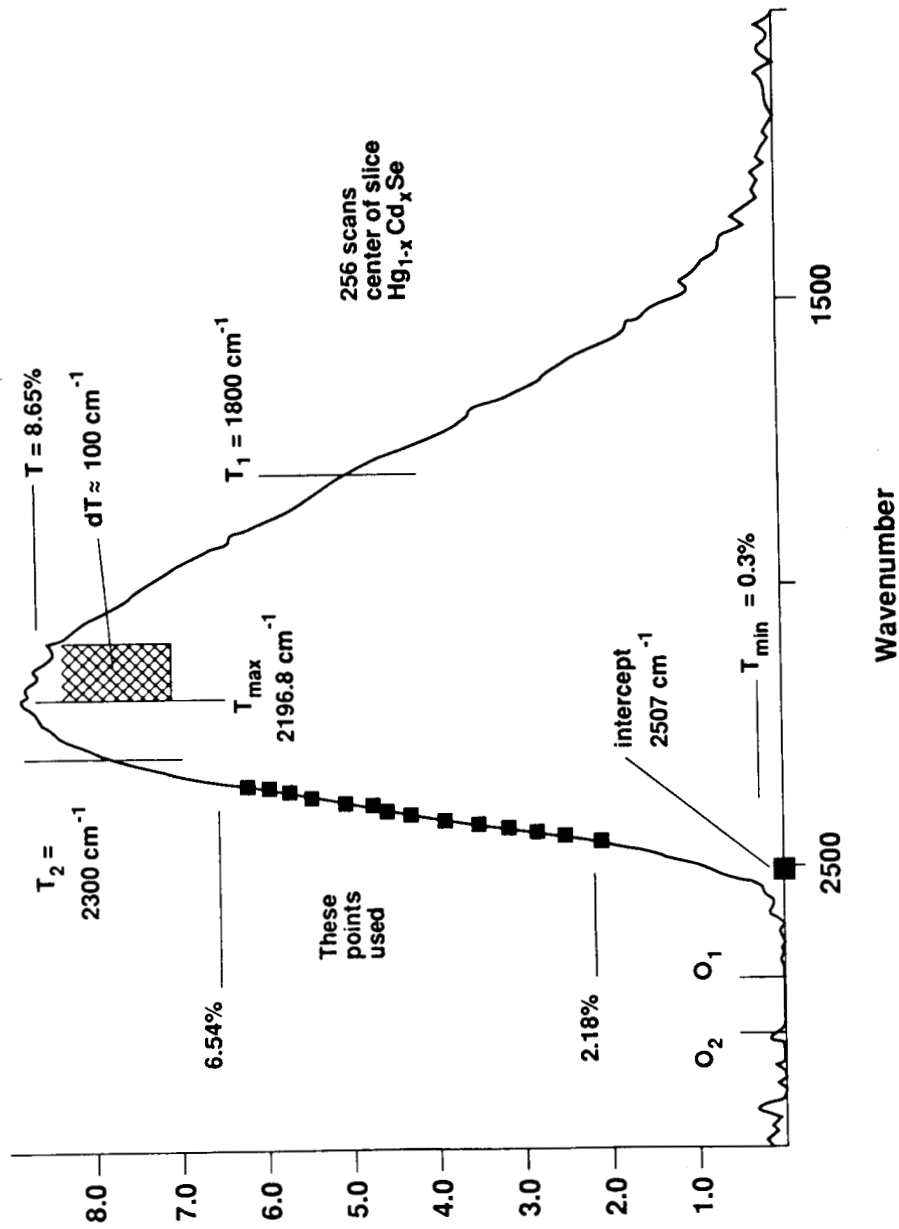
Figure 1. Illustration showing the use of the algorithm for extracting the cut-on wavelength from a semiconductor transmission spectrum. The spectral resolution is 16 cm^{-1}.
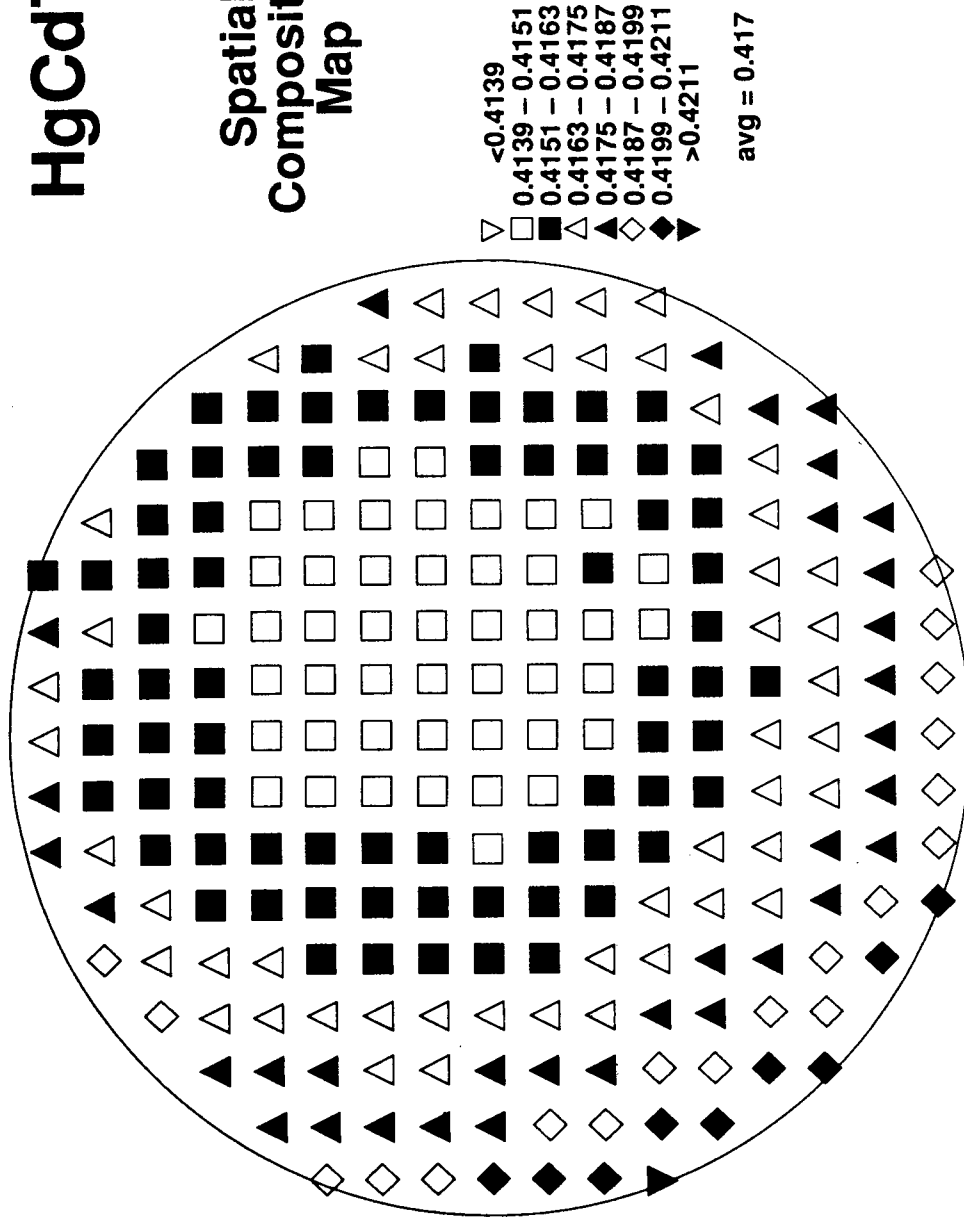
Figure 2. Spatial composition map of a unidirectionally solidified sample of $Hg_{1-x}Cd_xTe$ cut perpendicular to the growth axis. The step size between points is 5 (250 μm), and each point represents the same area as the 100 μm diameter aperture.
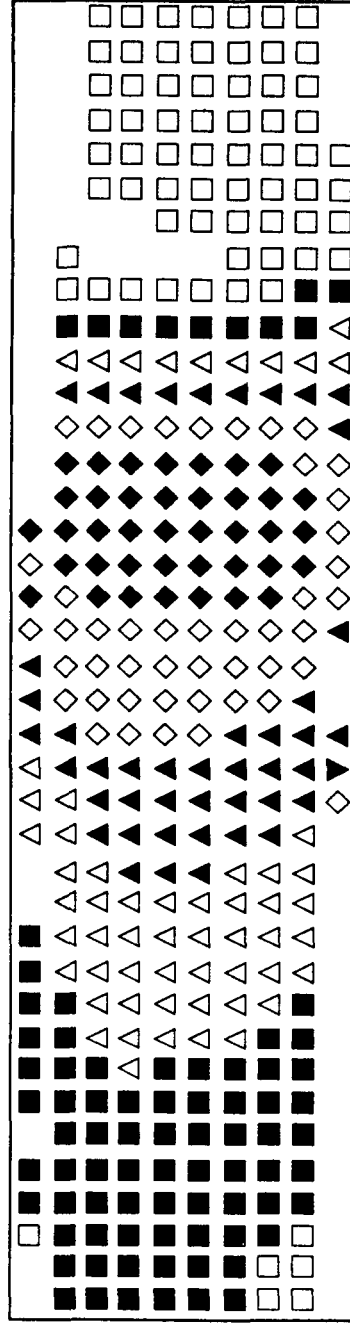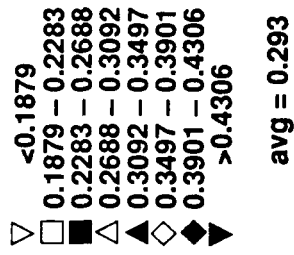
Figure 3. Spatial composition map of a unidirectionally solidified $Hg_{1-x}Cd_xSe$ wafer whose growth axis is horizontal from left to right. The step size between points is 10 (500 μm), and each point represents a 300 μm diameter aperture size.
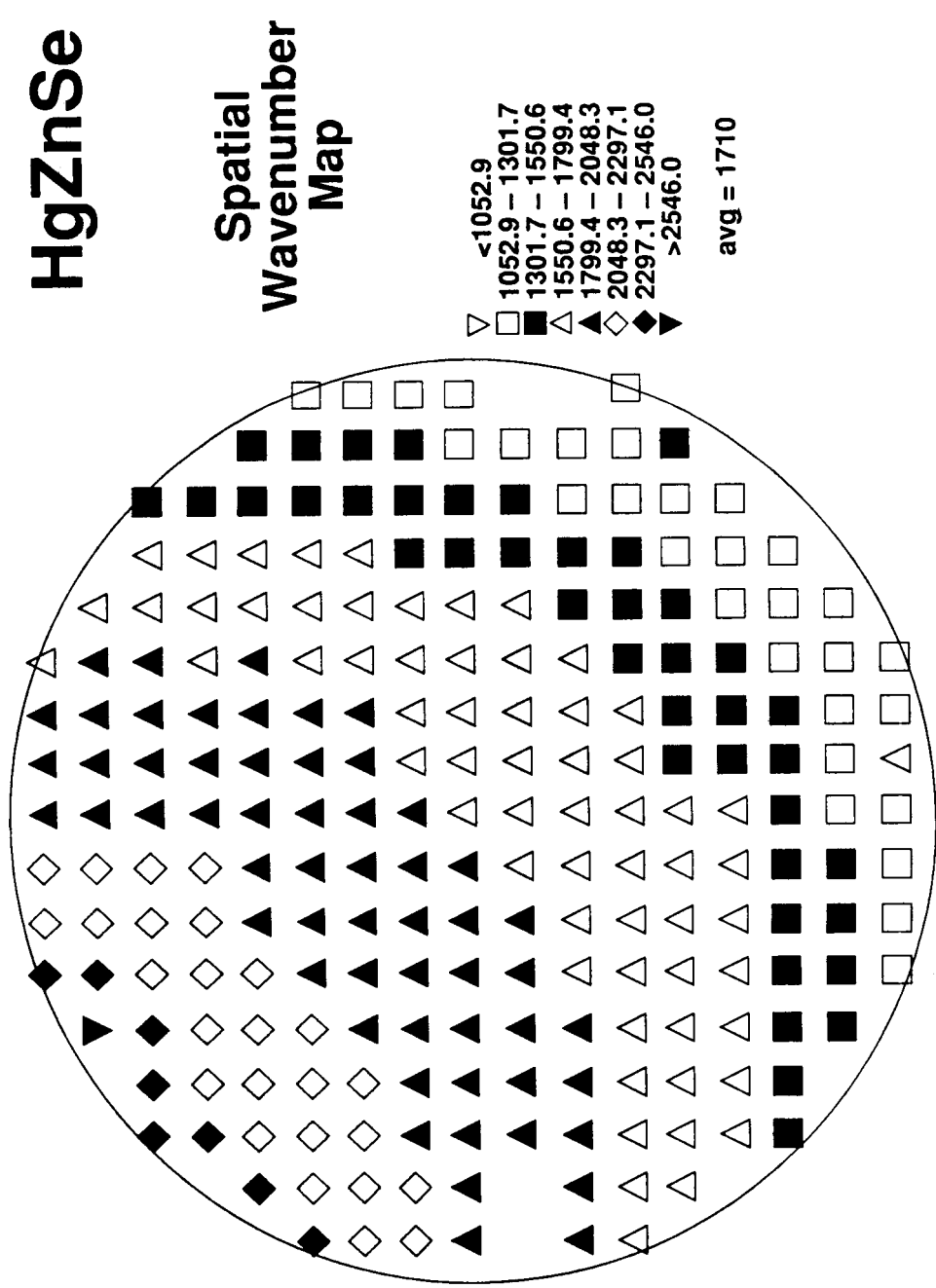
Figure 4. Spatial wavenumber map of a unidirectionally solidified $Hg_{1-x}Zn_xSe$ sample cut perpendicular to the growth axis. The step size between points is 5 (250 µm), and each point represents the same area as the 100 µm diameter aperture.
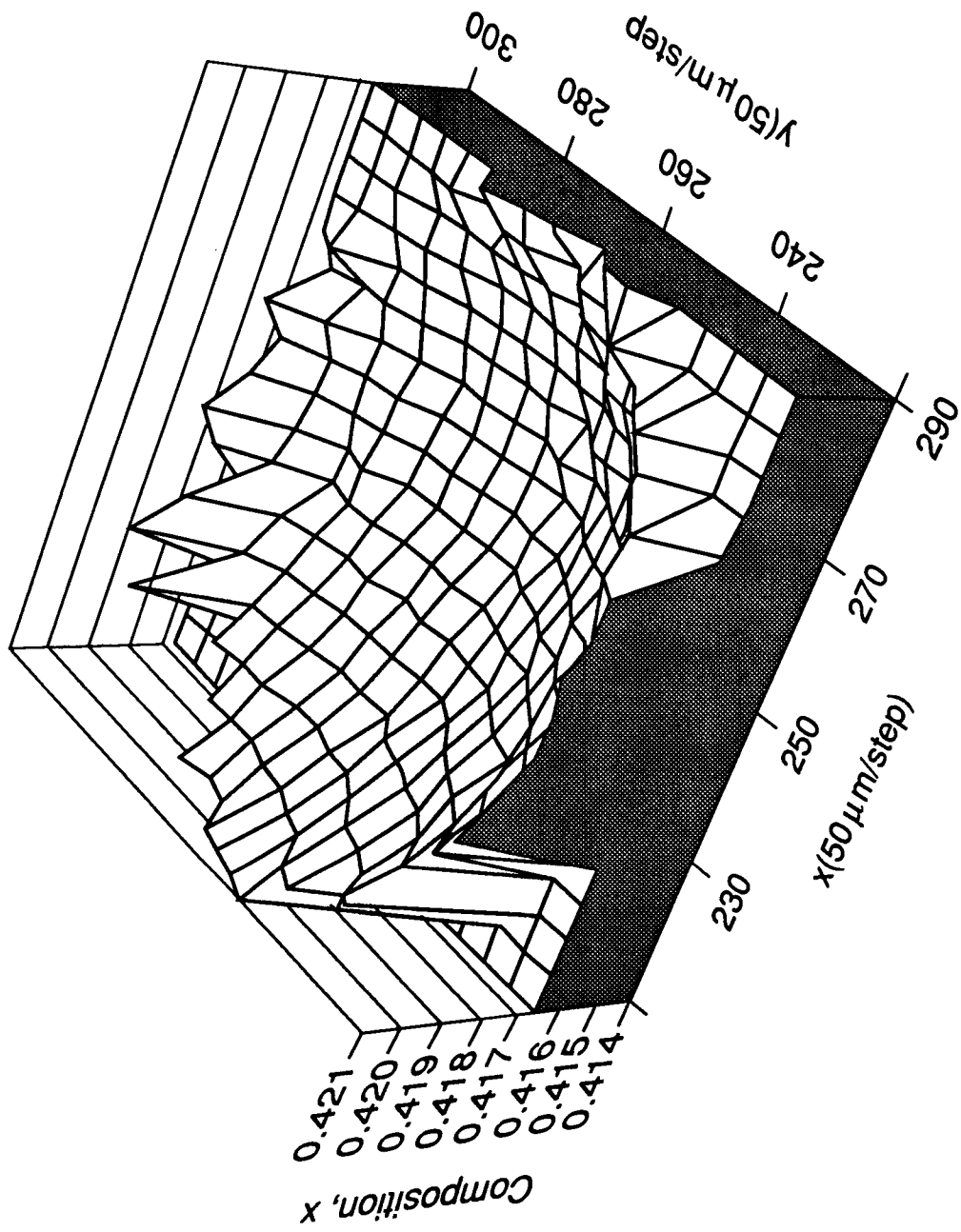
Figure 5. Three-dimensional plot of the compositions shown in Figure 2.

11
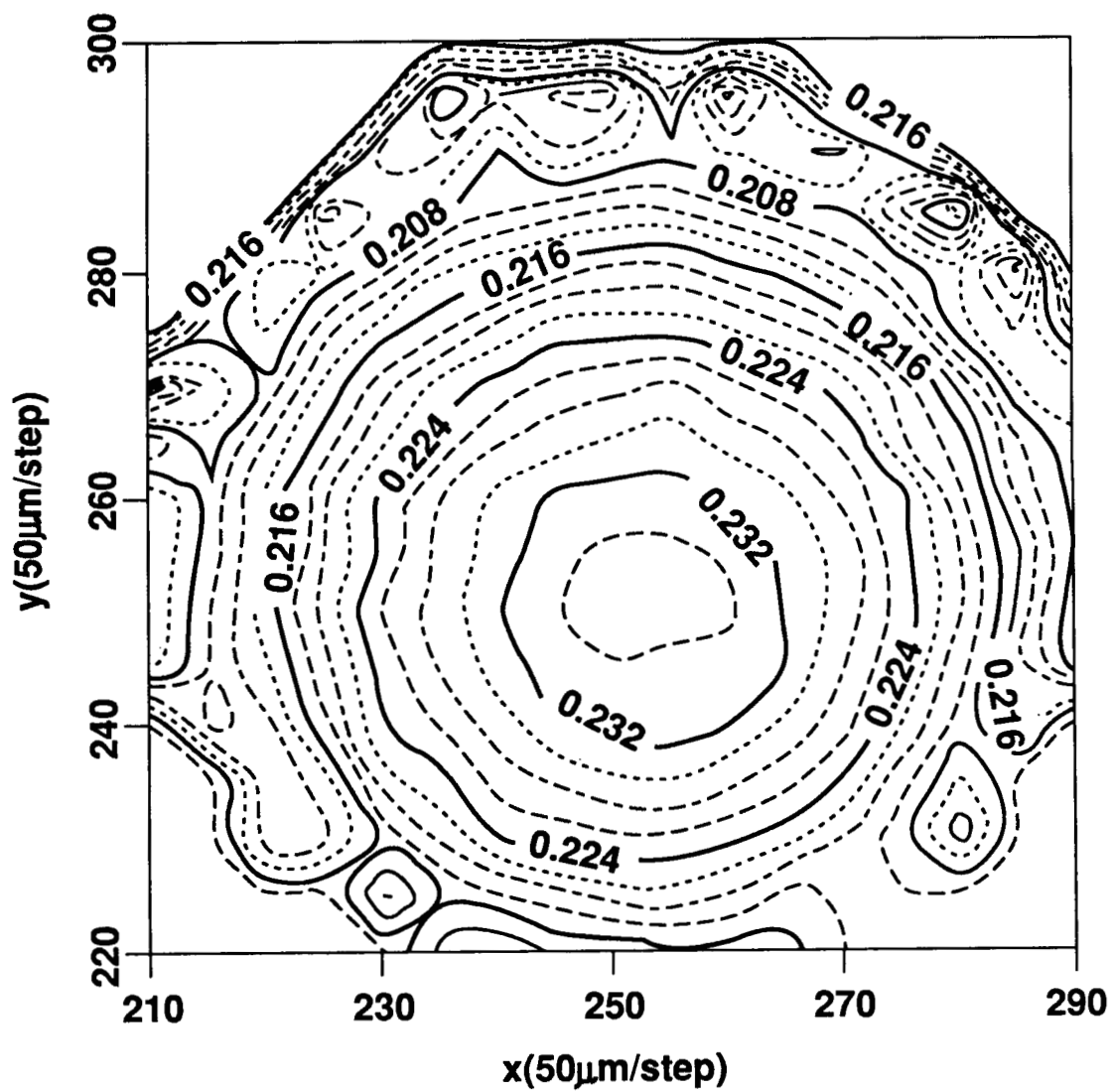
Figure 6. Contour map showing compositions of CdSe fraction, x, from a slice of $Hg_{1-x}Cd_xSe$. The sample size and grid size are the same as in Figure 5.
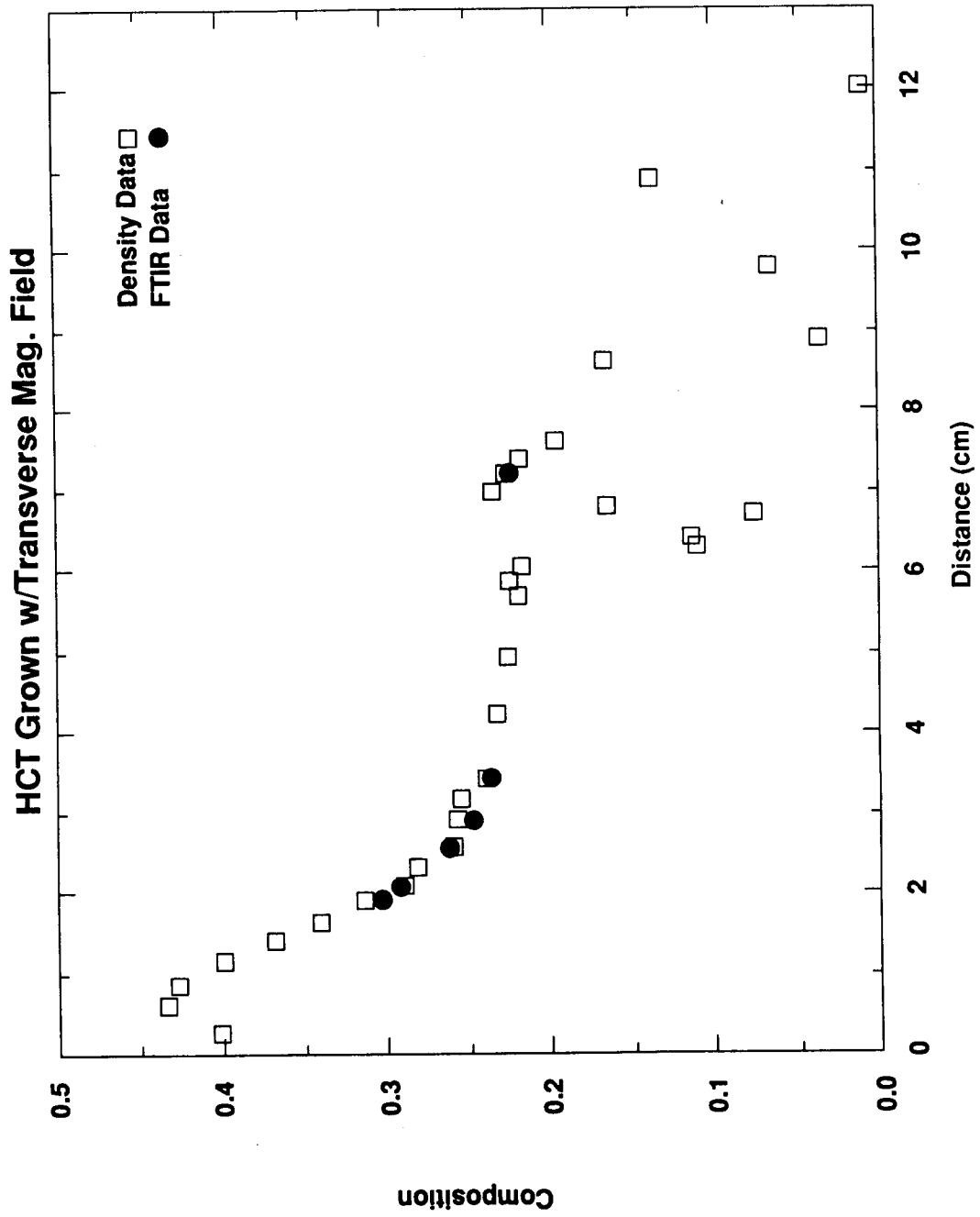
Figure 7. Plot showing the axial trend of CdTe composition, x, vs. distance of an ingot of $Hg_{1-x}Cd_xTe$ unidirectionally solidified using a transverse magnetic field. Both density measurement and FTIR data are shown.

13

TABLE 1. FTIR HEADER FILE PARAMETERS

1	apod triangle	apodization function (triangle or boxcar)
2	phasetype phaseapod	phase correction (phase, real, imaginary or power)
3	xstart 4000.0	starting wavenumber for graph
4	xend 400.0	ending wavenumber for graph
5	scale none	type of plot scaling (none or auto)
6	laseramp 2	sample every ith laser zero crossing (1 - 16)
7	color red	color for the plot
8	datasize w	size of data (w : 32 bit words s : 16 bit words)
9	axescolor green	color for the axes
10	datatype ras	default file extension
11	bkgscl 0	scaling applied to .big file (not to be modified)
12	sampscl 0	scaling applied to .igm file (not to be modified)
13	speed 2	plotting speed (0 - 4 with 0 the fastest)
14	ffsymmetry double	type of fft symmetry (double or single)
15	ymin 0.0	scaling for y-axis
16	ymax 1.0	scaling for y-axis (yin = ymax for auto scaling)
17	fvel 6	forward mirror velocity (1 - 7)
18	rvel 6	reverse mirror velocity (1 - 7)
19	lpf 0	low pass filter (0 - 8)
20	hpf 0	high pass filter (0 - 2)
21	sampdir forward	sampling direction (forward, reverse, or both)
22	fstart 399.0	starting wavenumber in file
23	fend 4001.0	ending wavenumber in file
24	spec-range MIR	spectrometer scanning range (FIR MIR NIR)
25	dend 2548	ending point of an interferogram plot
26	dstart 0	starting point of an interferogram plot
27	nphzfft 512	number of phase fft points
28	nphzdata 256	number of points in phase array
29	nrawdata 2548	number of input data points (nrawdata > ndata)
30	nfft 4096	number of fft points (must be power of 2)
31	ndata 2048	number of data points used
32	nscans 256	number of scans to be co-added
33	nscnbkg 16	number of scans to be co-added for background
34	iris 50	iris opening size (%)
35	sgain 3	post amplifier gain (1 - 3)
36	title	'C2-H 2.40 cm'
37	det 3	detector selection (1 - 3)
38	material HgCdTe	type of material
39	shape 0	0 = circular and 1 = rectangular
40	apert 100	aperture diameter in micrometers
41	center 250 260	sample center in xy stage coordinates
42	radius 2.2	sample radius in cm
43	transp1 1000.0	wavenumber to begin searching for max. trans.
44	transp2 1500.0	wavenumber to stop searching for transmax
45	trinc 100.0	wavenumber increment (dT) to average for transmax
46	opaque1 2000.0	wavenumber to begin averaging for opaque transmittance
47	opaque2 2200.0	wavenumber to stop averaging for opaque transmittance
48	transmin 0.0030	do not calculate cut-on if transmittance<transmin

NOTE: Numbers 38–48 are the additional parameters used by the algorithm to extract cut-on wavelengths from transmission spectra.

14

APPROVAL

HIGHLY AUTOMATED OPTICAL CHARACTERIZATION WITH FTIR SPECTROMETRY

By G.L.E. Perry and F. R. Szofran

The information in this report has been reviewed for technical content. Review of any information concerning Department of Defense or nuclear energy activities or programs has been made by the MSFC Security Classification Officer. This report, in its entirety, has been determined to be unclassified.

E. TANDBERG-HANSSEN
Director
Space Science Laboratory